Reactions of Nickel(II) 2-Aza-5,10,15,20-tetraphenyl-21-carbaporphyrin with Methyl Iodide. The First Structural Characterization of a Paramagnetic Organometallic Nickel(II) Complex†

Piotr J. Chmielewski, Lechosław Latos-Grażyński,* and Tadeusz Głowiak

Contribution from the Department of Chemistry, University of Wrocław, 50 383 Wrocław, Poland

Received August 9, 1995⊗

Abstract: The methylation of a nickel(II) complex (CTPP)Ni^{II} of 2-aza-5,10,15,20-tetraphenyl-21-carbaporphyrin ($CTPPH_2$) with the mild methylating agent methyl iodide yields novel stable organonickel(II) complexes: diamagnetic (21-CH_3TPP)Ni^{II} and two scarce paramagnetic species (2-NH-21-CH_3CTPP)Ni^{II}X and (2-NCH_3-21-CH_3CTPP)Ni^{II}X (X = Cl, I). The demetalation procedure resulted in isolation of two 21-carbaporphyrin derivatives, methylated at the internal C(21) carbon atom, i.e., 2-aza-5,10,15,20-tetraphenyl-21-methyl-21-carbaporphyrin (21-CH_3-$CTPPH_2$) and 2-aza-2-methyl-5,10,15,20-tetraphenyl-21-methyl-21-carbaporphyrin (2-NCH_3-21-CH_3CTPPH). The methylation mechanism involves the oxidative addition of the methyl cation to the carbaporphyrin C(21) activated due to Ni−C coordination. These C-methylated macrocycles preserve their coordinating properties as the remetalation processes have been carried out. The reversible concerted addition of HX converts the diamagnetic (21-CH_3TPP)Ni^{II} into the paramagnetic (2-NH-21-CH_3CTPP)Ni^{II}X. The axial coordination step is accompanied by a protonation of the peripheral nitrogen. The structures of (21-CH_3CTPP)NI^{II} (monoclinic, $P2_1/c$; $a = 15.055(3)$ Å, $b = 15.795(3)$ Å, $c = 17.069(3)$ Å, $\beta = 115.00(3)°$, $Z = 4$, least-square refinement of 476 parameters using 3622 reflections, $R = 0.069$) and (2-NCH_3-21-CH_3CTPP)Ni^{II}I (monoclinic, $P2_1/n$; $a = 12.946(3)$ Å, $b = 23.519(5)$ Å, $c = 13.945$ Å; $\beta = 93.2(3)°$, $Z = 4$, the least-square refinement of 502 parameters using 3257 reflections, $R = 0.0559$) have been determined by X-ray diffraction. In the first case the nickel(II) is four-coordinate with bonds to three pyrrole nitrogen atoms (Ni−N distances 1.948(5); 1.955(5); 1.938(5) Å) and the pyrrole carbon (Ni−C 2.005(6) Å). The nickel lies in the plane of the three nitrogens, while the methylated pyrrole is sharply tilted out of the plane with dihedral angle between the plane of three nitrogens and the methylated pyrrole plane being −42.2°. The methylated pyrrole is bound to nickel *via* a pyramidal carbon in the η^1-fashion. The first structurally characterized paramagnetic organonickel(II) complex (2-NCH_3-21-CH_3CTPP)Ni^{II}I presents unique features related to its electronic structure. The nickel(II) is five-coordinate with bonds to three pyrrole nitrogen atoms (Ni−N distances 2.032(8); 2.057(8); 1.979(8) Å) and to the pyrrole C(21) carbon (Ni−C 2.406(9) Å). The nickel is moved out from the plane of the three nitrogen plane toward the iodide ligand. The 21-CH_3 group and iodide are located on the opposite sides of the macrocycle. The substituted pyrrole is sharply tilted out of the plane with the dihedral angle between the three nitrogen plane and the methylated pyrrole plane being −55.3°. The methylated pyrrole is bound to nickel in the η^1-fashion but the coordinating C(21) atom preserves features related to trigonal sp^2 hybridization. The angle between the inverted pyrrole plane and the Ni−C bond increases from 42.8° to 70.1° on moving from the diamagnetic to paramagnetic species. The ^{1}H NMR and ^{2}H NMR spectra of paramagnetic (2-NH-21-CH_3CTPP)Ni^{II}X and (2-NCH_3-21-CH_3CTPP)Ni^{II}X complexes have been examined. Functional group assignments have been made with use of selective deuteration and 2D COSY experiments. The characteristic patterns of six downfield shifted pyrrole resonances accompanied by upfield shifted 3-H and 2-NH resonances are diagnostic of C-methylation. The 21-CH_3 resonance appears in a characteristic 90−110 ppm region.

Introduction

The development of the polydentate ligands with the potential donor carbon atom favorably oriented toward the transition metal ion affords a new strategy for stabilization of organometallic compounds including their atypical oxidation states or unusual transition metal intermediates.[1−3] The metal−carbon bond can be firmly held in the cavity of the multidentate ligand such that the possible dissociation of the M−C bond will be impaired. The potentially terdentate monoanionic ligands [(2,6-Me_2NCH_2)-C_6H_3]$^-$ and α,α′-diphosphino-*m*-xylenes provide spectacular examples of such chemistry.[2,3] Intramolecular activation, which results in cyclometalation, received considerable interest in this respect.[3] The formation of the stable organometallic compounds may be supported by the prearranged structure of the macrocyclic ligand, for instance the introduction of a *m*-xylene group into the crown thioether framework produced 2,6,10-trithia[11]-*m*-cyclophane which acted as a tetradentate ligand toward palladium. The precoordination by other donor centers of this polydentate ligand enhances an activation of the C−H bond. Thus this macrocycle coordinates through three S donors and the C(2) carbon of the xylene moiety.[4]

† Abbreviations used: CTPP ($CTPPH_2$) 2-aza-5,10,15,20-tetraphenyl-21-carbaporphyrin dianion; 2-NCH_3CTPP (2-NCH_3CTPPH) 2-aza-2-methyl-5,10,15,20-tetraphenyl-21-carbaporphyrin dianion; 21-CH_3CTPP (21-CH_3-$CTPPH_2$) 2-aza-5,10,15,20-tetraphenyl-21-methyl-21-carbaporphyrin dianion; 2-NH-21-CH_3CTPP (2-NH-21-CH_3CTTPH) 2-aza-5,10,15,20-tetraphenyl-21-methyl-21-carbaporphyrin monoanion; 2-NCH_3-21-CH_3CTTP (2-NCH_3-21-CH_3CTPPH) 2-aza-2,21-dimethyl-5,10,15,20-tetraphenyl-21-carbaporphyrin monoanion; TPP ($TPPH_2$), 5,10,15,20-tetraphenylporphyrin dianion, NCH_3TPP (NCH_3TPPH), 5,10,15,20-tetraphenyl-21-methylporphyrin monoanion; OEP ($OEPH_2$) octaethylporphyrin dianion; NCH_3OEP (NCH_3OEPH) *N*-methyloctaethylporphyrin monoanion. The abbreviations for the neutral forms are given in parentheses.

⊗ Abstract published in *Advance ACS Abstracts,* May 15, 1996.

S0002-7863(95)02702-8 CCC: $12.00

Van Koten et al. demonstrated that the [(2,6-Me_2NCH_2)-C_6H_3]$^-$ ligand stabilized the unique organometallic Ni(III) complex.[1c−e] The remarkably low Ni^{II}/Ni^{III} redox potentials[1c−e,k] of {[(2,6-Me_2NCH_2)C_6H_3]Ni^{II}}X originate catalytic reactivity in the Kharasch addition reaction, i.e., the 1:1 addition of polyhalogenated alkanes to alkenes with formation of new C−C and C−X bonds. Homogenous catalysts related to heterogeneous ones based on soluble polymeric supports[1j] or silane dendrimers[11] functionalized with pendant arylnickel(II) complexes have been explored as well.

Organometallic chemistry of nickel is of current interest in connection with mechanism of reactions of metalloenzymes which contain the nickel ion, e.g., methyl-*S*-coenzyme-M reductase and carbon monoxide dehydrogenase.[5−9] Organonickel complexes have been included as crucial intermediates in both enzymatic cycles. In general organonickel(II) complexes are diamagnetic including uncommon derivatives of nickel(II) porphyrins.[10] Paramagnetic organonickel(II) compounds are extremely rare and for a very long period of time have been exemplified by (σ-methyl)nickel(II)[(*R*,*R*,*S*,*S*)-N,N′,N″,N‴-tetramethylcyclam].[11] Recently a paramagnetic σ-methyl derivative of F430 (a nickel(II) tetrapyrrole whose structure corresponds to that of hydrocorphin) was prepared by *in situ* methylation.[12] In the same time the axial coordination of σ-phenyl to nickel(II) to produce paramagnetic complexes with 21-thiaporphyrin or 21-*N*-methylporphyrin as equatorial ligands were demonstrated as well.[13]

Chart 1

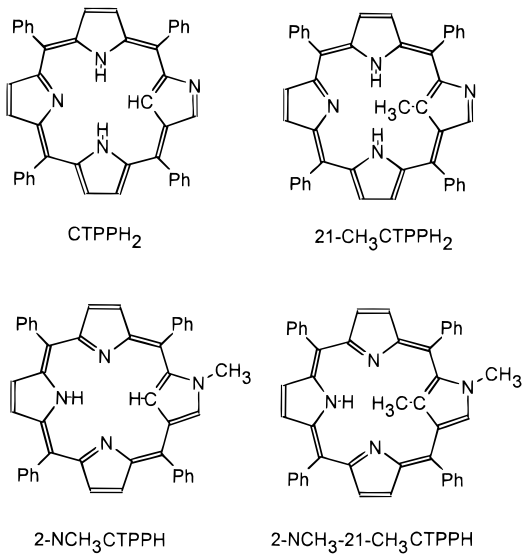

In the context of organometallic chemistry of nickel(II) facilitated by the appropriate construction of the polydentate macrocycle, we have focused on porphyrin-related ligands, i.e., 2-aza-5,10,15,20-tetraphenyl-21-carbaporphyrin and 2-*N*-methyl-5,10,15,20-tetraphenyl-21-carbaporphyrin. These ligands are isomers of their regular counterparts, i.e., of 5,10,15,20-tetraphenylporphyrin and 5,10,15,20-tetraphenyl-21-*N*-methylporphyrin and are formed formally by an inversion of pyrrole or N-methylated pyrrole rings.[14−16] With the replacement of the pyrrolenine nitrogen by a methine group, a carbaporphyrin molecule retains coordination properties as demonstrated recently by the formation of diamagnetic nickel(II) complexes, i.e., (CTPP)Ni^{II} and (2-NCH_3CTPP)Ni^{II}.[14,16] $CTPPH_2$ and 2-NCH_3CTPPH are geometrically similar to $TPPH_2$ and potentially offer a suitable fit to a variety of metal ions. The structural constraints typical for metalloporphyrins may be instrumental in stabilization of their metallocarbaporphyrin counterparts resulting in a peculiar stabilization of a σ-metal−carbon bond.[14,16] The unusual lability of the inner C−H bond is a prerequisite of the 21-carbaporphyrin coordination to produce the relatively robust Ni^{II}−C bond.

In the course of the mild methylation of $CTPPH_2$ we have identified the derivative methylated exclusively at the ligand periphery.[16] Here we have sought to extend our investigation from the methylation of 21-carbaporphyrin to its nickel(II) complex.

As a part of our continuing program of investigating the general relationship between the isotropic shift pattern and the molecular and electronic structures of paramagnetic nickel(II) porphyrins[13,17−19] we now report on the synthesis and characterization of mono- and dimethylated nickel(II) carbaporphyrins. In particular this work demonstrates that it is conceivable to stabilize high-spin organonickel(II) macrocyclic complex with

(1) (a) de Koster, A.; Kanters, J. A.; Spek, A. L.; van der Zeijden, A. A. H.; van Koten, G.; Vrieze, K. *Acta Crystallogr*. **1985**, *C41*, 893. (b) Grove, D. M.; van Koten, G.; Ubbels, H. J. C.; Zoet, R.; Spek, A. L. *Organometallics* **1984**, *3*, 1003. (c) Grove, D. M.; van Koten, G.; Zoet, R.; Murrall, N. W.; Welch, A. J. *J. Am. Chem. Soc.* **1983**, *105*, 1379. (d) Grove, D. M.; van Koten, G.; Mul, P.; Zoet, R.; van der Linden, J. G. M.; Legters, J.; Schmitz, J. E. J.; Murrall, N. W.; Welch, A. J. *Inorg. Chem.* **1988**, *27*, 2466. (e) Grove, D. M.; van Koten, G.; Mul, W. P.; van der Zeijden, A. A. H.; Terheiden, J.; Zoutberg, M. C.; Stam, C. H. *Organometallics* **1986**, *5*, 322. (f) Grove, D. M.; van Koten, G.; Louwen, J. N.; Noltes, J. G.; Spek, A. L.; Ubbels, H. J. C. *J. Am. Chem. Soc.* **1982**, *104*, 6609. (g) Abbenhuis, H. C. L.; Feiken, N.; Haarman, H. F.; Grove, D. M.; Horn, E.; Kooijman, H.; Spek, A. L.; van Koten, G. *Angew. Chem., Int. Ed. Engl.* **1991**, *30*, 996. (h) Grove, D. M.; van Koten, G.; Verschuuren, A. H. M. *J. Mol. Catal.* **1988**, *45*, 169. (i) Grove, D. M.; Verschuuren, A. H. M.; van Koten, G.; van Beek, J. A. M. *J. Organomet. Chem.* **1989**, *372*, C1. (j) van de Kuil, L. A.; Grove, D. M.; Zwikker, J. W.; Jenneskens, L. W.; Drenth, W.; van Koten, G. *Chem. Mater.* **1994**, *8*, 1675. (k) van de Kuil, L. A.; Luitjes, H.; Grove, D. M.; Zwikker, J. W.; van der Linden, J. G. M.; Roelofsen, A. M.; Jenneskens, L. W.; Drenth, W.; van Koten, G. *Organometallics* **1994**, *13*, 468. (l) Knapen, J. W. J.; van der Made, A. W.; de Wilde, J. C.; van Leeuwen, P. W. N. M.; Wijkens, P.; Grove, D. M.; van Koten, G. *Nature* **1994**, *372*, 659. (m) Terheijden, J.; van Koten, G.; Vinke, I. C.; Spek, A. L. *J. Am. Chem. Soc.* **1985**, *107*, 2891.

(2) (a) Moulton, C. J.; Saw, B. L. *J. Chem. Soc., Dalton Trans.* **1976**, 1020. (b) Rimml, H.; Venanzi, L. M. *J. Organomet. Chem.* **1983**, *259*, C6. (c) Nemeh, S.; Jensen, C.; Binamira-Soriaga, E.; Kaska, W. C. *Organometallics* **1983**, *2*, 1422. (d) Gozin, M.; Weisman, A.; Ben-David, Y.; Milstein, D. *Nature* **1993**, *364*, 699. (e) Liou, S.-Y.; Gozin, M.; Milstein, D. *J. Chem. Soc., Chem. Commun.* **1995**, 1965.

(3) Newkome, G. R.; Puckett, W. E.; Gupta, V. K.; Kiefer, G. E. *Chem. Rev.* **1986**, *86*, 451.

(4) Giesbrecht, G. R.; Hanan, G. S.; Kickham, J. E.; Loeb, S. J. *Inorg. Chem.* **1992**, *31*, 3286.

(5) Jaun, B. *Helv. Chim. Acta.* **1990**, *73*, 2209.

(6) Lu, W. P.; Harder, S. R.; Ragsdale, S. W. *Biochemistry* **1990**, *265*, 3124.

(7) Halcrow, M. A.; Christou, G. *Chem. Rev.* **1994**, *94*, 2421.

(8) (a) Pfaltz, A. In *The Bioinorganic Chemistry of Nickel*; Lancaster, J. R., Jr.; Ed., VCH Publishers, Inc.: New York, 1988; p 275. (b) Jaun, B. In *Metal Ions in Biological Systems*; Sigel, H., Sigel, A., Eds.; Marcel Dekker, Inc.: New York, 1993; Vol. 29, p 287.

(9) Stavropoulos, P.; Muetterties, M. C.; Carrié, Holm, R. H. *J. Am. Chem. Soc.* **1991**, *113*, 8485.

(10) (a) Chevrier, B.; Weiss, R. *J. Am. Chem. Soc.* **1976**, *98*, 2985. (b) Callot, H. J.; Chevrier, B.; Weiss, R. *J. Am. Chem. Soc.* **1978**, *100*, 4773.

(11) D'Aniello, M. J., Jr.; Barefield, E. K. *J. Am. Chem. Soc.* **1976**, *98*, 1610.

(12) Lin, S.-K.; Jaun, B. *Helv. Chim. Acta.* **1991**, *74*, 1725.

(13) Chmielewski, P. J.; Latos-Grażyński, L. *Inorg. Chem.* **1992**, *31*, 5231.

(14) (a) First reported by Chmielewski, P. J. and Latos-Grażyński, L. at 12th Summer School on Coordination Chemistry, Karpacz, Poland 1993. (b) Chmielewski, P. J.; Latos-Grażyński, L.; Rachlewicz, K.; Głowiak, T. *Angew. Chem., Int. Ed. Engl.* **1994**, *33*, 779.

(15) Furuta, H.; Asano, T.; Ogawa, T. *J. Am. Chem. Soc.* **1994**, *116*, 767.

(16) Chmielewski, P. J.; Latos-Grażyński, L. *J. Chem. Soc., Perkin Trans. 2* **1995**, 503.

(17) Latos-Grażyński, L. *Inorg. Chem.* **1985**, *24*, 1681.

(18) (a) Lisowski, J.; Latos-Grażyński, L.; Szterenberg, L. *Inorg. Chem.* **1992**, *31*, 933.

(19) Chmielewski, P. J.; Latos-Grażyński, L.; Pacholska, E. *Inorg. Chem.* **1994**, *33*, 1992.

an equatorial nickel−carbon bond. The first structural characterization of paramagnetic organonickel(II) complexes has been also accomplished.

Results and Discussion

Formation of Mono- and Dimethylated Nickel(II) Carbaporphyrins. Methylation of (CTPP)Ni^{II} has been performed in chloroform or dichloromethane solution using methyl iodide. In spite of the (CTPP)Ni^{II} reactivity toward methyl iodide its stability in chlorinated solvents has been observed. Preliminary studies involved introduction of methyl iodide into a chloroform-*d* solution of (CTPP)Ni^{II} (30:1 molar ratio). Since the ^{1}H NMR spectra of nickel(II) porphyrins and heteroporphyrins offer a sensitive technique for distinguishing between various spin/oxidation/ligation states[13,17−20] it has been used as the principal method for following the methylation pattern and the progress of the reaction. "Finger print" resonances of the 21-CH_3, 2-NH, and 2-N-CH_3 groups are located out of the crowded diamagnetic region and were readily detected. The ^{1}H NMR changes are consistent with the preference for methylation at the internal C(21) position followed subsequently by the reaction at the peripheral N(2) nitrogen. A variation in the relative concentrations of monomethylated and dimethylated derivatives has been observed over 7 days. The C-monomethylated species dominated the reaction products after 24 h of the reaction. Eventually the reaction resulted in complete conversion to a dimethylated paramagnetic product. Concurrently the reaction progress was followed by chromatographic separation. We have found that the reaction route does not include the peripheral methylation as the first step to form (2-NCH_3CTPP)Ni^{II} in measurable yield. Previously we have demonstrated that methylation of $CTPPH_2$ with methyl iodide proceeded exclusively at the outer N(2) position and that insertion of the nickel(II) in this macrocycle was readily achieved to produce diamagnetic (2-NCH_3CTPP)Ni^{II}.[16] Furthermore, in an independent experiment we have found that treatment of (2-NCH_3-CTPP)Ni^{II} with methyl iodide in chloroform (292 K, 1:50 molar ratio) results in the methylation of the C(21) position, yielding practically quantitatively as determined by the ^{1}H NMR, dimethylated paramagnetic nickel(II) complexes after 2 days of reaction. Once the optimal conditions were determined the way was open toward isolation of the new compounds.

Methylation of (CTPP)Ni^{II} carried out on the synthetic scale lead to isolation of mono- and dimethylated species, i.e., (21-CH_3CTPP)Ni^{II}, (2-NH-21-CH_3CTPP)Ni^{II}Cl, and (2-NCH_3-21-CH_3CTPP)Ni^{II}Cl. The resulting complexes have good solubility in dichloromethane, chloroform, and toluene. In the solid state and in solution these complexes are air stable and can be chromatographed. The feasible spontaneous demethylation process to end up with (CTPP)Ni^{II} or (2-NCH_3CTPP)Ni^{II}, demonstrated previously for N-methylated analogue (NCH_3-TPP)Ni^{II}Cl, has not been detected.[17] It has ruled out the possibility of the activation of a carbon−carbon bond by nickel insertion[2d,e] even though C(21)−CH_3 bond is favorably oriented toward the Ni^{II} ion.

The electronic absorption spectra of (21-CH_3CTPP)Ni^{II}, (2-NH-21-CH_3CTPP)Ni^{II}Cl, and (2-NCH_3-21-CH_3CTPP)Ni^{II}Cl are presented in Figure 1. Methylated complexes have spectral characteristics that resemble those of regular metalloporphyrins. Thus the intense feature at ca. 450 nm corresponds to the porphyrin Soret band, and the weaker features in the visible region are related to the porphyrin Q-band absorption. The (2-NH-21-CH_3CTPP)Ni^{II}Cl and (2-NCH_3-21-CH_3CTPP)Ni^{II}Cl complexes are paramagnetic as demonstrated by their distinctive isotropic shift of pyrrole and phenyl resonances (vide infra).

(20) La Mar, G.; Walker, F. A. In *Porphyrins*; Dolphin, D., Ed.; Academic Press: New York, 1979; Vol. IVB, p 61.

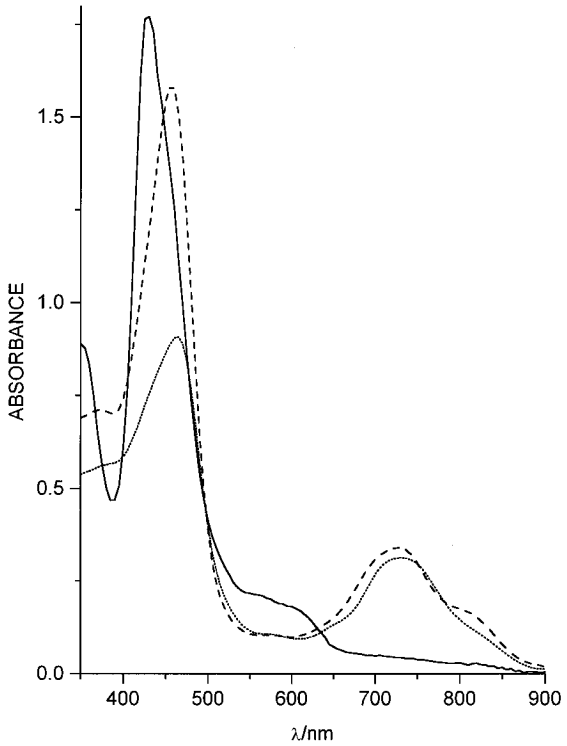

Figure 1. UV−vis spectra of the methylated nickel(II) carbaporphyrins (dichloromethane, 293 K): solid line, (21-CH_3CTPP)Ni^{II}; dashed line; (2-NH-21-CH_3CTPP)Ni^{II}Cl; dotted line, (2-NCH_3-21-CH_3CTPP)Ni^{II}Cl.

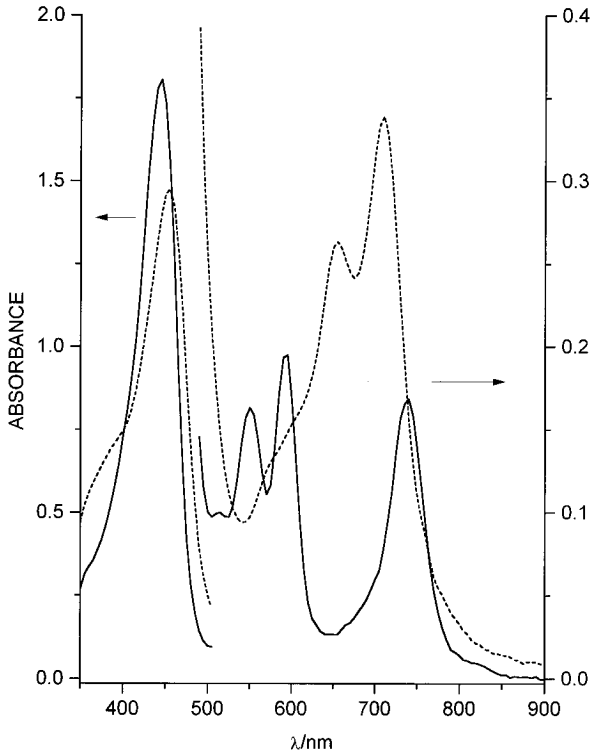

Figure 2. UV−vis spectra of the methylated carbaporphyrins (dichloromethane, 293 K): solid line, 21-CH_3CTPPH_2; dashed line, 2-NCH_3-21-CH_3CTPPH.

The identification of ligands has been confirmed by the parallel investigation of the acidic demetalation products of (21-CH_3CTPP)Ni^{II} and (2-NCH_3-21-CH_3CTPP)Ni^{II}Cl to obtain 21-CH_3CTPPH_2 and 2-NCH_3-21-CH_3CTPPH, respectively. The electronic spectra of 21-CH_3CTPPH_2 and 2-NCH_3-21-CH_3-CTPPH are porphyrin-like with the most intense bands at 445 and 455 nm, respectively, corresponding to the Soret band of the regular porphyrin and are shown in Figure 2. The ^{1}H NMR

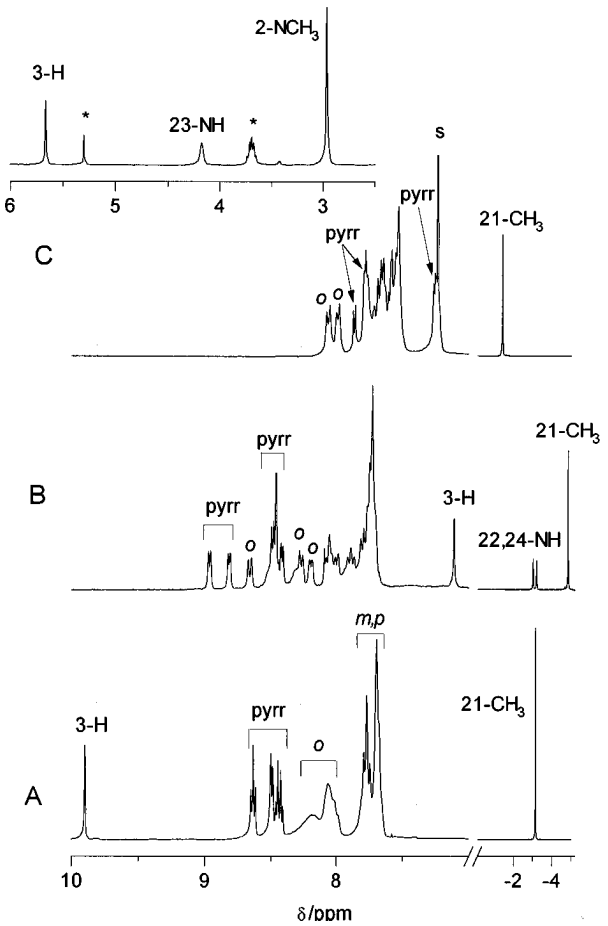

Figure 3. 300 MHz ^{1}H NMR spectra of (21-CH_3CTPP)Ni^{II} (trace A, dichloromethane-d_2, 293 K), 21-CH_3CTPPH_2 (trace B, dichloromethane-d_2, 203 K), and 2-NCH_3-21-CH_3CTPPH (trace C, chloroform-*d*, 223 K). Peak labels follow systematic position numbering of the porphyrin ring or denote proton groups: pyrr, regular pyrrole ring protons; *o*, *m*, and *p*—*ortho*, *meta*, and *para* protons of *meso*-phenyl ring, respectively; s, solvent. Asterisk mark solvents present in the crystal lattice of 2-NCH_3-21-CH_3CTPPH.

spectrum of 21-CH_3CTPPH_2 shows three AB patterns of the pyrrole protons (Figure 3). The fourth inverted C-methylated pyrrole ring shows a CH_3 singlet in the unique position of −4.837 ppm. This shift is consistent with the position of the *N*-methyl resonances of the regular N-methylated porphyrins.[21] Thus the 21-CH_3 upfield chemical shift is clearly associated with its location in the inner core of the carbaporphyrin. The methyl group is exposed to the strong shielding effect produced by the ring current effect. The spectrum of 21-CH_3CTPPH_2 resembles one analyzed previously in detail for CTPPH_2, admitting the fact that the strongly upfield shifted 21-H resonance has been replaced by the resonance with intensity of three protons unambiguously assigned to 21-CH_3.[14−16] Two resonances of deuterium exchangeable 22-NH and 24-NH protons have been also identified at −3.02 and −3.20 ppm (CD_2Cl_2, 203 K). The ^{1}H NMR spectrum of 2-NCH_3-21-CH_3-CTPPH is presented in trace C of Figure 3. In comparison to 21-CH_3CTPPH_2 we have observed considerable smaller values of all chemical shifts including the 21-CH_3 signal at −1.398 ppm. In addition we have identified only a single 23-NH resonances at 4.18 ppm ($CDCl_3$, 223 K). The peripheral methylation resulted with the 2-NCH_3 resonance at 2.972 ppm. The tautomeric structures, shown in Chart 1, prevail in the solution for the newly isolated ligands. The close similarities of the ^{1}H NMR spectra have been observed in pairs between CTPPH_2 and 21-CH_3CTPPH_2 or 2-NCH_3CTPPH and 2-NCH_3-21-CH_3CTPPH, respectively.

Both methylated carbaporphyrins preserve some degree of aromaticity. All outer pyrrole and phenyl resonances demonstrate downfield shifts due to ring current effect. The upfield shifts have been determined for 21-CH_3 and inner NH protons. However, the ring current shifts decrease considerably on going from 21-CH_3CTPPH_2 to 2-NCH_3-21-CH_3CTPPH or as previously found[16] on going from CTPPH_2 to 2-NCH_3-CTPPH. Accordingly the lowering of aromaticity is due to the external methylation.

Different tautomeric forms may also be invoked to account for the pyramidal coordination and the possible anionic nature of the C(21) atom of methylated carbaporphyrin. Hypothetical tautomers in Chart 2 are conveniently prearranged for coordination and demonstrate strongly marked pyramidal nature of the C(21) carbon. Two inner protons, 21-CH and 23-NH of 21-H-21-CH_3CTPPH, are available for dissociation to create a dianion. Only the inner 21-CH of 2-NH-21-CH_3CTPP or 2-NCH_3-21-H-21-CH_3CTPP may dissociate to generate a monoanionic environment. Such tautomers have not been experimentally encountered as uncoordinated structures but represent the useful presentation of the feasible coordination modes (*vide infra*).

The ^{1}H NMR spectrum of diamagnetic (21-CH_3CTPP)Ni^{II} (trace A in Figure 3) demonstrates the very characteristic feature of the upfield shifted C-methyl resonances in close analogy to diamagnetic N-methylated metalloporphyrin[21] and provides evidence for the structural formula as below:

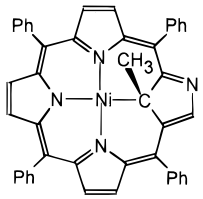

This structural formula favors the π delocalization *via* the outer porphyrin path as established also in the corresponding crystal structure (vide infra), while in 21-CH_3CTPPH_2 the inner and outer delocalization routes can act simultaneously. Consequently the remarkable increase of the ring current effect in the C-methylated pyrrolic fragment of (21-CH_3CTPP)Ni^{II}, reflected by the remarkable chemical shift of the 3-H resonance, has been demonstrated. Finally, we have found that both isolated ligands 21-CH_3CTPPH_2 and 2-NCH_3-21-CH_3CTPPH are susceptible to facile nickel(II) insertion giving as products (21-CH_3CTPP)-Ni^{II} and (2-NCH_3-21-CH_3CTPP)Ni^{II}Cl, respectively.

Crystal and Molecular Structure of (21-CH_3CTPP)Ni^{II}. The structure of (21-CH_3CTPP)Ni^{II} has been determined by X-ray crystallography. Table 1 contains selected bond distances and angles. The structure suffers from disorder that involves the location of the peripheral nitrogen atom and the adjacent carbon atom. Thus N(2) and C(3) share a common position. It has been refined to give 50% occupancy. Figure 4 shows the perspective view of the complex with the disorder removed. The crystal contains also one disordered molecule of dichloromethane. The Ni−N distances are comparable to those in the nearly planar diamagnetic (OEP)Ni^{II} complex (1.958(2) Å)[22] in the triclinic form and are consistent with the averaged distances 1.955(3) Å and 1.963(3) Å determined for disordered (CTTP)Ni^{II}.[14] These distances are slightly longer than those found for four-coordinate nickel(II) porphyrin, i.e., the tetragonal modification of (OEP)Ni^{II} (1.929(3) Å);[23] nickel(II) tetraphe-

(21) Lavallee, D. K. *The Chemistry and Biochemistry of N-substituted Porphyrins*; VCH Publishers: New York, 1987.
(22) Cullen, D. R.; Meyer, E. F. Jr. *J. Am. Chem. Soc.* **1974**, *96*, 2095.
(23) Meyer, E. F., Jr. *Acta Crystallogr.* **1972**, *B28*, 2162.

Chart 2

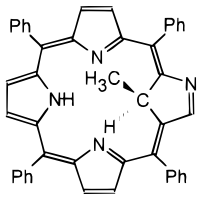

21-H-21-CH_3CTPPH

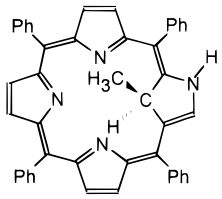

2-NH-21-H-21-CH_3CTPPH

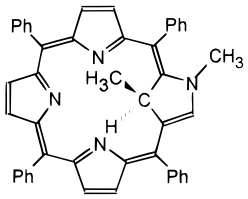

2-NCH_3-21-H-21-CH_3CTPPH

Table 1. Selected Bond Lengths (Å) and Angles (deg) for (21-CH_3CTPP)Ni^{II} and (2-NCH_3-21-CH_3CTPP)Ni^{II}I

Bond Lengths (Å)

	(21-CH_3TPP)Ni^{II}	(2-NCH_3-21-CH_3TPP)Ni^{II}I
Ni−N(24)	1.948(5)	2.032(8)
Ni−N(22)	1.955(5)	2.057(8)
Ni−N(23)	1.938(5)	1.979(8)
Ni−C(21)	2.005(6)	2.406(9)
C(21)−C(25)	1.541(9)	1.53(2)
C(21)−C(4)	1.468(9)	1.41(2)
C(21)−C(1)	1.480(8)	1.390(14)
C(3)−C(4)	1.392(9)	1.407(14)
N(2)−C(3)	1.344(9)	1.332(14)
N(2)−C(1)	1.372(9)	1.406(14)

Bond Angles (deg)

	(21-CH_3CTPP)Ni^{II}	(2-NCH_3-21-CH_3CTPP)Ni^{II}I
C(21)−Ni−N(23)	176.6(2)	154.2(4)
N(22)−Ni−N(24)	173.8(2)	158.4(4)
C(21)−Ni−N(24)	88.8(2)	84.8(4)
C(21)−Ni−N(22)	88.5(2)	85.3(3)
N(24)−Ni−N(23)	91.4(2)	90.9(3)
N(23)−Ni−N(22)	91.0(2)	89.8(3)
Ni−C(21)−C(25)	94.8(4)	87.2(6)
Ni−C(21)−C(1)	117.6(4)	101.0(7)
Ni−C(21)−C(4)	118.2(4)	101.4(7)
C(1)−C(21)−C(25)	113.1(5)	125.0(11)
C(4)−C(21)−C(25)	113.8(5)	125.0(9)
C(1)−C(21)−C(4)	100.2(5)	106.7(9)
N(2)−C(1)−C(21)	111.5(6)	107.8(10)
C(3)−N(2)−C(1)	108.3(6)	109.3(9)
C(4)−C(3)−N(2)	110.5(6)	108.7(10)
C(21)−C(4)−C(3)	109.6(5)	107.4(9)

nylporphyrin with ethoxycarbonylcarbene fragment inserted into Ni−N bond (1.92(1) Å),[10a] *N*-tosylamino-5,10,15,20-tetraphenylporphyrinatonickel(II) (1.920(3), 1.883(3), 1.920(3) Å),[10b] and nickel(II) complexes of octaethylporphyrin *N*-oxide dianion (1.922(4), 1.900(4), 1.929(5) Å).[24]

The Ni−C bond length 2.005(6) Å in (21-CH_3CTPP)Ni^{II} is in the upper limits of Ni(II)−C bond lengths (1.81−2.02 Å).[1b,25−27] This bond is essentially longer than one determined for the constrained van Koten's nickel(II) system [(2,6-Me_2-$NCH_2)_2C_6H_3$]Ni^{II}(HCOO) 1.814(2) Å.[1b] The Ni^{II}−C bond length suggests sp^3 hybridization of the coordinating C(21) carbon atom. The determined distance is in good agreement with those found for the plain examples of the low spin nickel(II)−sp^3 hybridized carbon atom coordination, e.g., a simple alkyl derivative in a square planar nickel(II) complex (1.94(1) Å),[26] and nickel(II) complexes derived from the tripoidal ligands [$(N(CH_2CH_2S$-*iso*-$C_3H_7)_3Ni^{II}(CH_3)]^+$ 1.94(2) Å[9] and [$(N(CH_2CH_2P(C_6H_5)_2)_3Ni^{II}(CH_3)]^+$ 2.02(2) Å.[27]

The coordination core of (21-CH_3CTPP)Ni^{II} is essentially planar. Nickel(II) (0.097(1) Å) and C(21) (0.074(5) Å) are slightly displaced from the N(22)N(23)N(24) plane in the same direction. The shape of carbaporphyrin resembles that seen in metal complexes of *N*-alkylporphyrins. Contrary to the coordination center the macrocycle is far from being planar. The inverted C-methylated pyrrole is sharply tipped out of the N(22)N(23)N(24) plane. The *cis* and *trans* pyrrole rings are tilted in the reverse direction. Thus deviation of the pyrrole planes from the plane defined by N(22)N(23)N(24) are as follows: C(21) −42.2°, N(22) 15.4; N(23) 3.1°; N(24) 15.8°. Bending of the pyrrole ring allows this group to coordinate to the nickel(II) ion in an η^1 fashion through the C(21) carbon which acquires a pyramidal (sp^3-hybridized) geometry. Thus the metal lies out of the inverted pyrrole plane. The angle between the methylated pyrrole plane and the Ni^{II}−C(21) bond equals 42.0° and between the same plane and the C(21)−C(25) bond equals 52°. The perfect tetrahedral arrangement would produce ca. 55° inclination of these bonds.

Comparison of bond distances within the pyrrole and inverted methylated pyrrole portions demonstrates that extensive delocalization exists through the macrocycle and extends to the inverted pyrrole fragment. Bond distances of the regular pyrroles $C_\alpha-C_\beta > C_\alpha-C_{meso} > C_\alpha-C_N > C_\beta-C_\beta$ reproduce the pattern of the regular porphyrin ligands. There is appreciable effect of the aromatic character of the macrocycle on the inverted C-methylated pyrrole fragment. So N(2)−C(3), N(2)−C(1), and C(3)−C(4) bond distances are markedly shorter than C(1)−C(21) and C(4)−C(21). The C(21) atom approaches sp^3 hybridization geometrical parameters as illustrated by respective bond angles and distances presented in Table 1. The pattern of bond lengths within this fragment of the macrocycle is modified to allow π-delocalization *via* the outer path. The longer C(1)−C(21) and C(4)−C(21) bond distances are accounted for by the $sp^2 \rightarrow sp^3$ hybridization change due to C-methylation. This type of coordination is related to that of η^1-cyclopentadienyl complexes in which the metal−carbon bond displays a sp^3 hybridization geometry and the angle between the M−C bond and the C_5 plane is ca. 50°. The structural features of the inverted pyrrole ring are remarkably similar to the corresponding ones for monohaptocyclopentadienyl ring(s) in $(C_5H_5)_3MoNO$, $(C_5H_5)_4Ti$, and $(C_5H_5)_4Zr$ complexes.[28] For instance in the case of $(C_5H_5)_4Ti$ C−C bond length of η^1-C_5H_5 vary systematically around the ring in a manner consistent with the diene structure (starting at the carbon atom bound to Ti): 1.446(5), 1.360(6), 1.420(5), 1.355(6), and 1.442(5) Å. The C(2)−C(1)−C(5) angle at the coordinating carbon C(1) is 105.2(2)°. The Ti−C(1)−C(2) and Ti−C(1)−C(5) angles are equal 106.4(1)° and 114.1(1)°.[28b] No relevant nickel(II) por-

(24) Balch, A. L.; Chan, Y.-W.; Olmstead, M. M. *J. Am. Chem. Soc.* **1985**, *107*, 6510.

(25) Jolly, P. W. In *Comprehensive Organometallic Chemistry*; Wilkinson, G., Stone, F. G. A., Abel, E. W., Eds.; Pergamon: Oxford, 1982; Vol. 6, p 37.

(26) Barnett, B. L.; Kruger, C. *J. Organomet. Chem.* **1972**, *32*, 1699.

(27) Sacconi, L.; Dapporto, P.; Stoppioni, P.; Innocenti, P.; Benneli, C. *Inorg. Chem.* **1977**, *16*, 1669.

(28) (a) Calderon, J. L.; Cotton, F. A.; Legzdins, P. *J. Am. Chem. Soc.* **1969**, *91*, 2528. (b) Calderon, J. L.; Cotton, F. A.; DeBoer, B. G.; Takats, J. *J. Am. Chem. Soc.* **1971**, *93*, 3592. (c) Rogers, R. D.; Bynum, R. V.; Atwood, J. L. *J. Am. Chem. Soc.* **1978**, *100*, 5239.

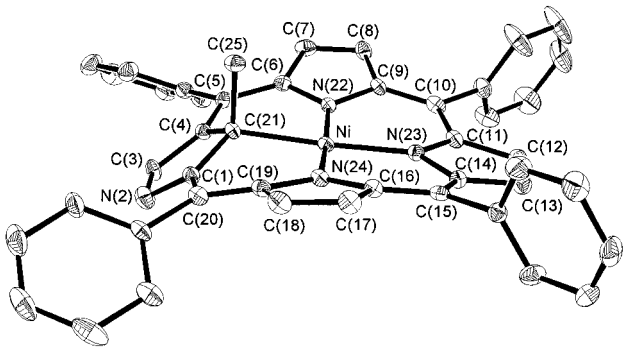

Figure 4. The perspective drawing of (21-CH_3CTPP)Ni^{II} showing one of the two equally possible molecule orientation with respect to the N(2)−C(3) permutation.

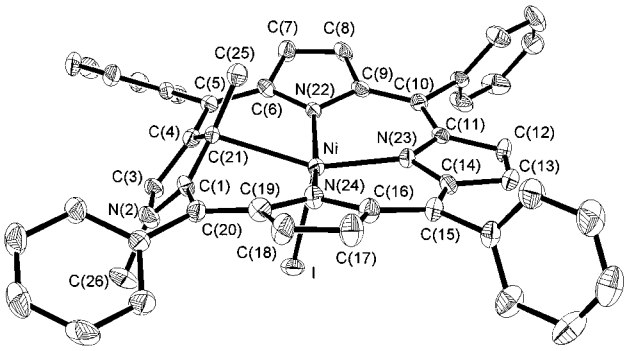

Figure 5. The perspective drawing of (2-NCH_3-21-CH_3CTPP)Ni^{II}I presenting the more abundant molecule orientation with respect to the N(2)−C(3) disorder.

phyrin structure seems to be available for direct comparisons with (21-CH_3CTPP)Ni^{II}. However the geometry of (21-CH_3-CTPP)Ni^{II} bears some resemblance to the coordination mode of N-methylated porphyrins where N-methylated pyrrole ring is strongly tipped off to afford coordination of the sp^3 hybridized nitrogen atom of the N-methylated pyrrole ring.[21]

Crystal and Molecular Structure of (2-NCH_3-21-CH_3-CTPP)Ni^{II}I. The structure of (2-NCH_3-21-CH_3CTPP)Ni^{II}I has been studied by X-ray diffraction. The perspective view of the complex which has no crystallographically imposed symmetry is shown in Figure 5. A selection of important bond distances and angles is included in Table 1 to compare with analogous values of the diamagnetic (21-CH_3CTPP)Ni^{II} species. The structure displays disorder in the location of the 2-NCH_3 fragment. The structure has been refined to give 65% occupancy with 2-NCH_3 as shown in Figure 5 and 35% occupancy with methyl group attached to the nitrogen atom replacing C(3) of the major form. Figure 5 only shows the major form. The unit cell also contains one molecule of benzene. The C-methyl substituent lies on the face opposite to the iodide. The nickel is displaced 0.375(2) Å out the N(22)N(23)N(24) plane toward the axial iodide. The deviation of the pyrrole planes from the plane defined by dihedral angles between the pyrrole and N(22)N(23)N(24) planes are as follows: C(21) −55.3°, N(22) 14.3°, N(23) 0.9°, N(24) 14.4°. The Ni−N bond lengths are longer than those found for (21-CH_3CTPP)Ni^{II} or other diamagnetic nickel(II) porphyrins but are similar to that 2.038(4) Å seen in a six-coordinate, high-spin nickel(II) porphyrin complex[29] or 2.09 Å in a six-coordinate high-spin nickel(II) hydroporphyrin complex.[30] The similarity of bond lengths to those found for the five-coordinate, high-spin nickel(II) tetraphenyl-21-thiaporphyrin 2.094(3), 1.963(3), 2.084(3) Å[31] has been also noted. The Ni^{II}−N distance of the Ni−N bond located opposite to C(21) is the shortest in the set in analogy to the (STPP)Ni^{II}Cl structure where the bond length to the nitrogen *trans* to the coordinating sulfur is the smallest.

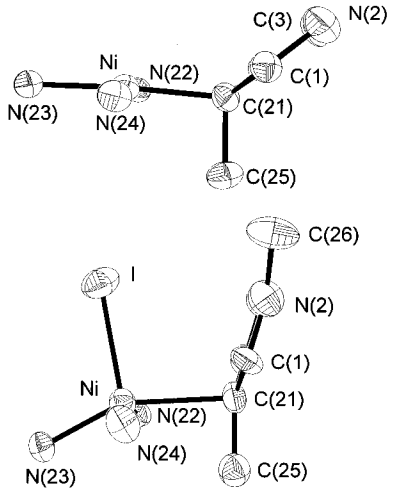

Figure 6. Comparison of nickel and C(21) environment geometry in (21-CH_3CTPP)Ni^{II} (upper drawing) and (2-NCH_3-21-CH_3CTPP)Ni^{II}I (lower drawing).

The C-methylated carbaporphyrin has had to rearrange profoundly in relation to (21-CH_3CTPP)Ni^{II} in order to accommodate the high-spin nickel(II) ion in the coordination crevice. The unprecedented structure demonstrates the methylated pyrrole ring sharply bent from the core plane defined here by the N(22)N(23)N(24) nitrogens, while the other pyrrole rings are slightly bent in the opposite direction. The angle between the C(1)C(21)C(4) and N(22)N(23)N(24) planes is −55.3° in the high-spin complex but −42.2° in the low-spin one. The methylated pyrrole ring is strongly bent out from the core plane preserving the planarity of the C-methylated pyrrole. Thus the N(2)−CH_3 and C(21)−CH_3 methyl groups lies near the methylated pyrrole plane with the angles between this plane and the corresponding bonds being 17.1° and −11.0°, respectively. Such an architecture allows coordination to the nickel(II) ion in an η^1 fashion through the C(21) carbon atom. Thus the metal lays out of the pyrrole plane, with the angle between the methylated pyrrole plane and the Ni^{II}−C(21) bond being 70.1° (Figure 6). However the carbon atom does not acquire a pyramidal geometry that is well defined for (21-CH_3CTPP)Ni^{II}. The coordinating carbon preserves planar trigonal geometry with some degree of pyramidal distortion, pointing out the considerable preservation of sp^2 hybridization. This suggests the bond formation due to the σ-accepting properties of the Ni^{II} from the p_z orbital of the sp^2 hybridized C(21) carbon. A comparison of the bonding geometry between (21-CH_3CTPP)Ni^{II} and (2-NCH_3-21-CH_3CTPP)Ni^{II}I is clearly demonstrated in Figure 6 and in Table 1. In order to get a more quantitative measure of the distortion we have decided to analyze the sum of the bond angles $\sum_1$ = Ni−C(21)−C(1) + Ni−C(21)−C(4) + Ni−C(21)−C(25) formed by the Ni−C(21) bond and $\sum_2$ = C(1)−C(21)−C(4) + C(1)−C(21)−C(25) + C(4)−C(21)−C(25) which describes the ligand planarity around the C(21) carbon. The comparison of the idealized geometries with (21-CH_3-CTPP)Ni^{II} and (2-NCH_3-21-CH_3CTPP)Ni^{II}I structures is given in Table 2.

The observed tendency to shorten the C(1)−C(21) and C(4)−C(21) bond distances within the inverted methylated pyrrole on going from (21-CH_3CTPP)Ni^{II} to (2-NCH_3-21-CH_3CTPP)-Ni^{II}I (Table 1) reveals the extensive π delocalization in

(29) Kirner, J. F.; Garofolo, J. Jr.; Scheidt, W. R. *Inorg. Nucl. Chem. Lett.* **1975**, *11*, 107.

(30) Kratky, C.; Fässler, A.; Pfaltz, A.; Kräutler, B.; Jaun, B.; Eschenmoser, A. *J. Chem. Soc., Chem. Commun.* **1984**, 1368.

Table 2. Comparison of Geometry around the Coordinating Carbon

		sum of bond angles (deg)	
		Σ_1	Σ_2
idealized geometry[a]	tetrahedral	328.5	328.5
	p_z side-on-fashion	270	360
crystal structure[a,b]	(21-CH_3CTPP)Ni^{II}	330.3	327.3
	(2-NCH_3-21-CH_3CTPP)Ni^{II}I	289.6	356.7
	$[IPtMeC_6H_3(CH_2NMe_2)_2$-2,6$]^+$	286.5	357.3
	[Pt(*o*-tolyl)$MeC_6H_3(CH_2NMe_2)_2$-2,6$]^+$	277.5	359.4

[a] Σ_1, Σ_2 of nickel(II) complexes defined in the text. [b] Σ_1 = Pt−C_{ipso}−C_{ortho} + Pt−C_{ipso}−$C_{ortho'}$ + Pt−C_{ipso}−C_{Me}; Σ_2 = C_{ortho}−C_{ipso}−$C_{ortho'}$ + C_{Me}−C_{ipso}−C_{ortho} + C_{Me}−C_{ipso}−$C_{ortho'}$.

(2-NCH_3-21-CH_3CTPP)Ni^{II}I *via* the inner route contrary to the (21-CH_3CTPP)Ni^{II} case where the availability of this path is limited.

The relevant structural rearrangement due to the methylation was established for C-methylated *trans*-2,6-bis[(dimethylamino)-methyl]phenyl-*N,C,N′* complex of platinum(II) [PtI(MeC_6H_3-$(CH_2NMe_2)_2$-*o,o′*)]$^+$ considered as an example of σ-metal substituted arenonium ion, in which the methyl group of the alkyl halide is bonded to the carbon atom of the aryl ring originally σ-bonded (sp^2-hybridized) to the platinum center.[1f] The angles between the plane defined by the coordinating C_{ipso} and two ortho carbons of the phenyl ring and the C−CH_3 and Pt−C bonds equal 16.0° and 93.4°, respectively. The angle between the C_{ipso}−CH_3 bond and the Pt−C_{ipso} bond is 104.2°. In the case of the [PtI(MeC_6H_3-$(CH_2NMe_2)_2$-*o,o′*)]$^+$ ([Pt(o-tolyl)(MeC_6H_3-$(CH_2NMe_2)_2$-*o,o′*)]$^+$) the Σ_1 and Σ_2 parameters suggest the relatively small tetrahedral distortion of C_{ipso} from the primary trigonal geometry and are rather consistent with the side-on coordination of the platinum cation (Table 2).[1f,m]

The Ni^{II}−C(21) distance (2.406(9) Å) seems to be unusually long, but we assume that it is still the bond distance. The Ni^{II}−C interaction may result from the proximity effect due to the location of the potential carbon donor at the macrocyclic structure. It has seemed reasonable to consider an alternative view of the bonding interaction which involves simultaneously more than one carbon atom.[36,37] The relevant relation of the nickel−carbon distances for high-spin [(Ni−C(21) 2.406(9) Å, Ni−C(25) 2.786 Å, Ni−C(4) 3.026 Å; Ni−C(1) 2.997 Å)] and low-spin [Ni−C(21) 2.005(6) Å; Ni−C(25) 2.629 Å; Ni−C(1) 2.986 Å; Ni−C(4) 2.988 Å)] complexes unambigously identify the C(21) atom as a center of the bonding interaction. The bonding interaction is manifested by a strong downfield isotropic shift of the 21-CH_3 group in the ^{1}H NMR spectra (*vide infra*). To the best of our knowledge the structure discussed here represents the very first structurally characterized case of high-spin organometallic Ni^{II} species. Consequently, we are not aware of any precedent for the typical high-spin Ni^{II}−C bond length. In our opinion the situation bears some distant resemblance, as far as bond lengths are concerned, to five-coordinate N-methylated porphyrin complexes of the metals of the first transition row. There, the N-methylated nitrogen−metal bonds fall in the range 2.257(5)−2.530(7) Å when the other regular M−N distances are markedly shorter.[21,32] Generally N-methylated porphyrins act as the monoanionic ligand stabilizing high-spin five coordinate complexes. The X-ray structure of (NCH_3TPP)Ni^{II}X has not been determined. It was found by means of ^{1}H NMR that this compound is paramagnetic and five-coordinate, similar to the (2-NH-21-CH_3CTPP)Ni^{II}Cl and (2-NCH_3-21-CH_3CTPP)Ni^{II}X (X = Cl^-, I^-) species investigated in this work.[13,17] It is truly remarkable that carbaporphyrin may adopt different geometries to accommodate high-spin or low-spin nickel(II) ions. The electron in the $d_{x^2-y^2}$ orbital greatly increases the effective radius of the nickel(II) ion. This fact easily accounts for the 0.05−0.1 Å increase of the Ni^{II}−N bond length going from low-spin to the high-spin species. Likewise, 0.12 Å increase of the axial Ni^{II}−N bond distance was determined for nickel(II) complexes with tripoidal ligands due to location of the unpaired electron at the d_{z^2} orbital.[9] Apart from the modification of the Ni^{II} effective ionic radius the dramatic change of the C(21) coordination mode is instrumental as well. As already discussed the geometry of C(21) coordination in (21-CH_3CTPP)Ni^{II} resembles a coordination of the anionic sp^3 hybridized alkyl ligand to the nickel(II) center. The side-on coordination of the inverted pyrrole demonstrates the novel type of coordination in the organometallic chemistry of high-spin nickel(II) with aromatic ligands.

Apart from the already mentioned σ-platinum substituted arenonium ion[1f,m] such a bonding mode has been encountered in the case of electrophilic interactions of silver salt with arenes.[33,34] An excellent example of η^1-coordination was offered by X-ray structure of a silver salt of the weakly coordinating carborane anion $B_{11}CH_{12}^-$ containing benzene in the lattice.[34] One benzene molecule coordinates to silver in the η^1-mode with the Ag−C_α distance of 2.400(7) Å and the Ag−C_α−C_β and Ag−C_α−$C_{\beta'}$ bond angles equal 89.5° and 94.6°, respectively (C_α—coordinating atom of benzene, C_β or $C_{\beta'}$ adjacent carbon atoms).

The other example of the peculiar interaction between cationic center and arene involves a structure of [$Et_3SiB(C_6F_5)_4$·toluene] where the silylium group is located directly above para-carbon of toluene in the side-on-fashion.[35] The description of the electronic structure is the matter of controversy, but it is considered in terms of an arenium cation [Et_3Si·toluene]$^+$.[35c] The existence of the covalent interaction between the Et_3Si group and the toluene has been recognized in spite of a long Si−C distance (2.18 Å).[35e]

NMR Studies of Paramagnetic Nickel(II) Complexes of Methylated Carbaporphyrin. The ^{1}H NMR data of the paramagnetic reaction products have been analyzed considering their C_1 symmetry which is adequate to described the methylated complexes (2-NH-21-CH_3CTPP)Ni^{II}Cl and (2-NCH_3-21-CH_3-CTPP)Ni^{II}Cl. There are seven distinct pyrrole positions for (2-NH-21-CH_3CTPP)Ni^{II}Cl, a 2-NH position analogous to the 2-CH of the regular porphyrin and four unequivalent meso phenyl rings. Respective NMR data for (2-NH-21-CH_3CTPP)-Ni^{II}Cl and (2-NCH_3-21-CH_3CTPP)Ni^{II}Cl are presented in Figures 7 and 8. The spectral parameters for these and other relevant compounds have been gathered in Table 3. Resonance assignments, which are given above each peak, have been made on the basis of relative intensities, line widths, site specific deuteration, and 2D COSY experiments. The most characteristic feature, the downfield broad resonance (line width 1320 Hz) at 109.7 ppm has been identified as the 21-CH_3 resonance. This resonance disappears in the ^{1}H NMR spectrum of (2-NH-21-

(31) Latos-Grażyński, L.; Lisowski, J.; Olmstead, M. M.; Balch, A. L. *Inorg. Chem.* **1989**, *28*, 1184.

(32) (a) Bartczak, T.; Latos-Grażyński, L.; Wysłouch, A. *Inorg. Chim. Acta* **1990**, *171*, 205. (b) Balch, A. L.; Cornman, C. R.; Latos-Grażyński, L.; Olmstead, M. M. *J. Am. Chem. Soc.* **1990**, *112*, 7552.

(33) Turner, R. W.; Amma, E. L. *J. Am. Chem. Soc.* **1966**, *88*, 3243. Hall Griffith, E. A.; Amma, E. L. *J. Am. Chem. Soc.* **1974**, *96*, 743.

(34) Shelly, K.; Finster, D. C.; Lee, Y. J.; Scheidt, W. R.; Reed, C. A. *J. Am. Chem. Soc.* **1985**, *107*, 5995.

(35) (a) Lambert, J. B.; Zhang, S.; Stern, C. L.; Huffman, J. C. *Science* **1993**, *260*, 1917. (b) Lambert, J. B.; Zhang, S. *Science* **1995**, *263*, 984. (c) von Ragué Schleyer, P.; Buzek, P.; Muller, T.; Apeloig, Y.; Siehl, H.-U. *Angew. Chem., Int. Ed. Engl.* **1993**, *32*, 1471. (d) Olah, G. A.; Rasul, G.; Li, X.-Y.; Bucholz, A.; Sandford, G.; Prakash, G. K. S. *Science* **1995**, *263*, 983. (e) Pauling, L. *Science* **1995**, *263*, 983. (f) Reed, C. A.; Xie, Z.; Bau, R.; Benesi, A. *Science* **1993**, *260*, 402. Reed, C. A.; Xie, Z. *Science* **1995**, *263*, 986. (g) Cacace, F.; Attiná, M.; Fornanrini, S. *Angew. Chem., Int. Ed. Engl.* **1995**, *34*, 654.

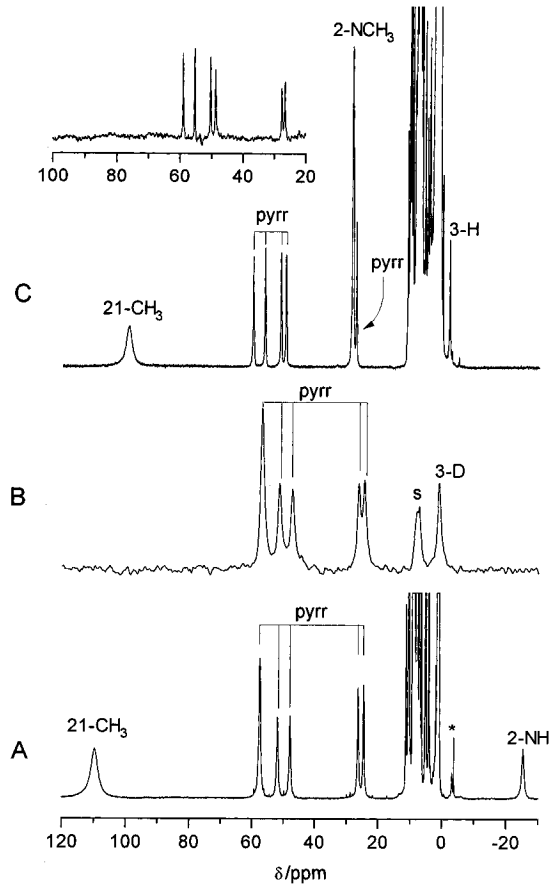

Figure 7. NMR spectra of paramagnetic mono- and dimethylated nickel(II) carbaporphyrin: (A) (2-NH-21-CH_3CTPP)$Ni^{II}Cl$ (^{1}H NMR, $CDCl_3$, 293 K); (B) (2-NH-21-CH_3CTPP-d_7)$Ni^{II}Cl$ (^{2}H NMR, $CHCl_3$, 293 K); (C) (2-NCH_3-21-CH_3CTPP)$Ni^{II}Cl$; inset (2-NCD_3-21-CD_3-CTPP)$Ni^{II}Cl$ (^{1}H NMR, $CDCl_3$, 293 K). Peak labels follow systematic numbering of the porphyrin ring or denote proton groups: pyrr, regular pyrrole ring protons; s, solvent. Asterisk marks traces of diamagnetic (21-CH_3CTPP)Ni^{II} found due to some 2-NH proton dissociation in solution.

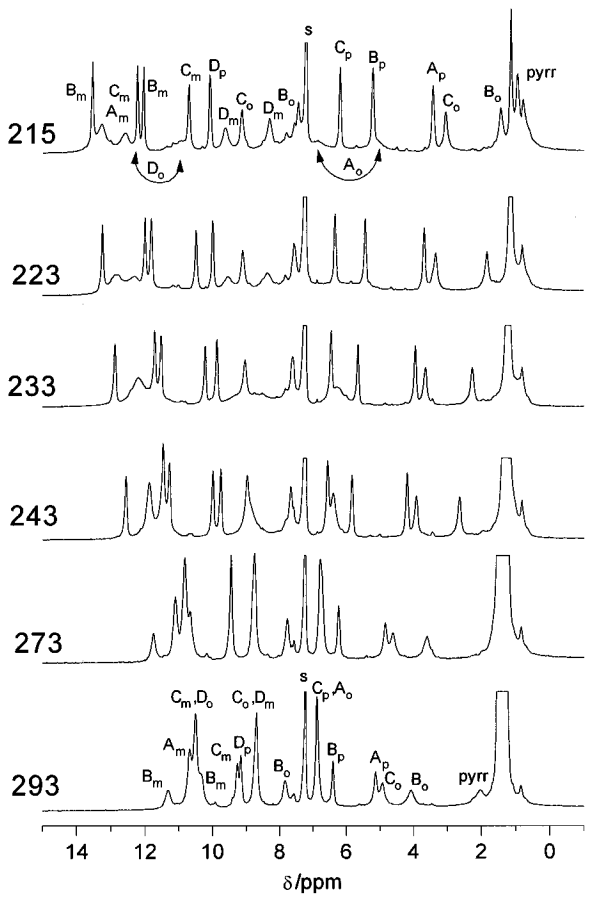

Figure 8. ^{1}H NMR spectra of the *meso*-phenyl region of (2-NH-21-CH_3CTPP)$Ni^{II}Cl$ in $CDCl_3$ at various temperatures. Peak labels denote respective *ortho*, *meta*, or *para* protons of unequivalent phenyl rings; s, solvent.

CD_3CTPP)$Ni^{II}Cl$. A resonance at −23.07 ppm (293 K) has been assigned to the 2-NH proton. This resonance is absent in the spectrum of (2-NCH_3-21-CH_3CTPP)$Ni^{II}Cl$. When chloroform-*d* saturated with deuterium oxide was added to the solution of (2-NH-21-CH_3CTPP)$Ni^{II}Cl$, the 2-NH resonance disappeared due to formation of (2-ND-21-CH_3CTPP)$Ni^{II}Cl$. In order to distinguish the pyrrole and phenyl resonances the ^{2}H NMR spectrum of (2-NH-21-CH_3CTPP-d_7)$Ni^{II}Cl$ has been obtained and is shown in trace B of Figure 7. The six pyrrole resonances are in the 60−20 ppm region. The single slightly upfield shifted pyrrole resonances at 2.04 ppm has been assigned to the 3-D position by analogy to (NCH_3TPP)$Ni^{II}Cl$.[13,17] The additional resonances, presented in detail in Figure 8, come from the *meso* phenyl protons. The resonance assignments of (2-NCH_3-21-CH_3CTPP)$Ni^{II}Cl$ follow that of (2-NH-21-CH_3CTPP)$Ni^{II}Cl$. The 2-NCH_3 resonance has been unambiguously identified since it is missing in the spectra of (2-NH-21-CH_3CTPP)$Ni^{II}Cl$ and (2-NCD_3-21-CD_3CTPP)$Ni^{II}Cl$ (Figure 8, Table 3).

The two-dimensional COSY experiment has been effective in connecting protons within pyrrole moieties and *meso* phenyl groups.[38] Figure 9 shows the representative COSY data of (2-NCH_3-21-CH_3CTPP)$Ni^{II}Cl$ gathered in chloroform-*d* solution at 273 K. Cross-peaks reveal pairwise coupling among six downfield pyrrole resonances. As expected no cross-peak has been seen for the upfield pyrrole resonance but this can be assigned to the 3-H position by default. Characteristic sets of cross-peaks due to coupling between five protons of a phenyl ring have been established and located in the COSY map for the four nonequivalent phenyls of (2-NCH_3-21-CH_3CTPP)$Ni^{II}Cl$. The results of these assignments were used to identify the individual resonances in Figures 8 and 9, and the resonance positions are given in Table 3 together with analogous data for (2-H-21-CH_3CTPP)$Ni^{II}Cl$. The two *ortho* and *meta* protons on each of the *meso*-phenyl rings are inequivalent since the porphyrin plane bears different substituents on the opposite sides and the rotation about the meso carbon−phenyl bond may be restricted. However, onset rotation about this bond will cause an exchange of these positions. Since all *meso* phenyl rings are structurally different and exposed to different steric hindrances, it is anticipated that there will be some differences in the rate of phenyl rotation for each ring type. The representative temperature dependence of the phenyl region for (2-H-21-CH_3-CTPP)$Ni^{II}Cl$ is shown in Figure 8. Two phenyls, labeled *B* and *C* demonstrated a set of five resonances typical for the slow rotation limit even at 293 K. The averaged features of three phenyl resonances have been seen for two other phenyls *A* and *D*. As the temperature lowered these *meta* and *ortho* resonances of *A* and *D* split due to slower rotation rate. At this stage we cannot assign the phenyls to the specific *meso* positions although the larger shift differences of the *ortho* resonances favor the tentative assignment of the B and C phenyls to the 5,20 positions which are close to the inverted pyrrole ring. The temperature dependent rotation of the *meso* phenyls have been observed for diamagnetic (21-CH_3CTPP)Ni^{II} as well.

(36) Crabtree, R. H. *Angew. Chem., Int. Ed. Engl.* **1993**, *32*, 654 and references cited therein.

(37) Kretz, C. M.; Gallo, E.; Sollari, E.; Floriani, C.; Chiesi-Villa, A.; Rizzoli, C. *J. Am. Chem. Soc.* **1994**, *116*, 10775 and references cited therein.

(38) Keating, K. A.; de Ropp, J. S.; La Mar, G. N.; Balch, A. L.; Shiau, F.-Y.; Smith, K. M. *Inorg. Chem.* **1991**, *30*, 3258.

Table 3. Chemical Shifts of Pyrrole Modified Nickel(II) Porphyrins

compound	chemical shifts, δ (ppm)								
	pyrrole			modified pyrrole	*o*-Ar	*m*-Ar	*p*-Ar	C(N)−Me	NH
(2-NH-21-CH_3CTTP)$Ni^{II}Cl^a$	58.06, 58.06	52.40, 48.25	26.53, 24.86	2.04 (3-H)	A 6.89 B 7.84, 4.09 C 8.70, 4.94 D 10.52	A 10.68 B11.33, 10.36 C 10.51, 9.27 D 8.70	A 5.11 B 6.41 C 6.89 D 9.16	109.70	−23.07 (2-NH)
(2-NCH_3-21-CH_3CTPP)$Ni^{II}Cl^a$	59.69[d] 55.95[e]	50.91[f] 49.33[f]	28.15[d] 27.16[e]	−2.03 (3-H)	A 7.61 B 8.36, 4.13 C 8.71, 4.79 D 9.91	A 10.29 B 11.04, 9.91 C 10.60, 9.40 D 9.40	A 5.64 B 6.55 C 6.79 D 8.22	98.81 28.30 (2-NCH_3)	
(2-NCH_3-21-CH_3CTPP)$Ni^{II}I^a$	58.79 55.39	50.08 47.88	24.25 23.86	−1.67 (3-H)	10.80, 10.28, 10.16, 9.98, 9.44, 8.95, 8.78, 8.01, 6.95, 6.29, 6.08, 4.65, 4.21			117.44 32.51 (2-NCH_3)	
(NCH_3TPP)$Ni^{II}Cl^b$ [17]	72.64	68.19	33.67	−9.84	8.44, 11.40, 5.91, 12.74	10.39, 10.84, 11.23, 9.14	8.01, 6.92	177.8	
(STPP)$Ni^{II}Cl^a$ [18a]	64.58[d]	32.51[d]	30.91	−29.84	7.31, 8.10	9.93, 9.81, 9.74	6.17, 6.53		
[(STPP)$Ni^{II}(CD_3OD)_2$]Cl^a [18a]	68.5[d]	36.0[d]	57.0	−22.0	9.42, 7.57	8.40, 9.92	8.57, 7.57		

[a] Chloroform-*d* solution, 293 K. [b] Chloroform-*d* solution, 213 K. [c] Methanol-d_4 293 K. [d–f] Pyrrole resonances pairwise scalar coupled; A, B, C, D resonance assigned to four unequivalent *meso* phenyl rings.

Table 4. Crystallographic Data for (21-CH_3CTPP)Ni^{II}·CH_2Cl_2 and (2-NCH_3-21-CH_3CTPP)$Ni^{II}I$·C_6H_6

compound	(21-CH_3CTPP)Ni^{II}·CH_2Cl_2	(2-NCH_3-21-CH_3CTPP)$Ni^{II}I$·C_6H_6
empirical formula	$C_{46}H_{32}N_4Cl_2Ni$	$C_{52}H_{39}N_4INi$
color, habit	brown prism	green prism
fw	770.38	905.50
crystal system	monoclinic	monoclinic
space group	$P2_1/c$	$P2_1/n$
a, Å	15.055(3)	12.946(3)
b, Å	15.795(3)	23.519(5)
c, Å	17.069(3)	13.945(3)
β, deg	115.00(3)	93.20(3)
V, Å^3	3679(1)	4239(2)
T, K	293(2)	293(2)
Z	4	4
crystal size, mm	0.05 × 0.1 × 0.20	0.08 × 0.1 × 0.12
d_{calcd}, g/cm^{-3}	1.391	1.419
radiation λ, Å	1.54180	1.54180
μ (Cu Kα), mm^{-1}	2.402	6.685
R_1[a]	0.0691	0.0559
wR_2[b]	0.1849	0.1433

[a] $R_1 = \sum||F_o| - |F_c||/\sum|F_o|$. [b] $wR_2 = [\sum[w(F_o^2 - F_c^2)^2]/\sum[w(F_o^2)^2]]^{1/2}$.

Analysis of Hyperfine Shifts. The Curie plots of the temperature dependencies of the chemical shifts of the pyrrole and methyl resonances of (2-NCH_3-21-CH_3CTPP)$Ni^{II}Cl$ and (2-NH-21-CH_3CTPP)$Ni^{II}Cl$ (not shown) demonstrate linear behavior with extrapolated intercepts that do not correspond to the suitable diamagnetic references (21-CH_3CTPP)Ni^{II} or relevant carbaporphyrin, indicating small contribution of the dipolar shift due to the anisotropy of zero-field splitting. The ZFS contribution presents the T^{-2} dependent curvature.[39,40] However, the alternate directions of phenyl shifts in (2-NH-21-CH_3-CTPP)$Ni^{II}Cl$ or (2-NCH_3-21-CH_3CTPP)$Ni^{II}Cl$ are compatible with the dominant π-contact contribution and negligible of the dipolar one. Analysis of the temperature dependence and of the phenyl isotropic shifts are in accord with dominance of contact contribution at the pyrrole positions. The dipolar mechanism in Ni^{II}(NCH_3TPP)Cl also contributed less than 10% to the pyrrole shifts.[17] The downfield shift of pyrrole and C-methyl resonances indicates a σ-delocalization of spin density. This is consistent with the ground state of Ni^{II} which has two unpaired electrons in the σ-symmetry orbitals $(d_{x^2-y^2})^1(d_{z^2})^1$.

The isotropic shift of the inverted C-methylated pyrrole ring is of a significant importance with respect to the nature of the interaction in this paramagnetic organometallic Ni^{II} complex and requires a special comment. The considerable downfield $C-CH_3$ shift can be accounted for by the direct σ-delocalization *via* three single bonds in the Ni−C(21)−C−H fragment. The directions and magnitudes of the shifts are close to those reported for (NCH_3TPP)$Ni^{II}Cl$ and (NCH_3OEP)$Ni^{II}Cl$ complexes.[13,17] The tilt of the inverted C-methylated ring changes the geometry of the spin density delocalization path as compared to the regular pyrrole rings. The unpaired spin density is localized on the molecular orbital dominated by the p_z component which can transfer the σ-spin density but simultaneously contributes to π-orbitals of the inverted pyrrole ring. Such an overlap within the inverted ring will permit the direct transfer of unpaired spin density of the C(21) p_z into the π system without any π M−L bonding.[17−19] The side-on-coordination of the C-methylated moiety folds the pathways of the spin delocalization. This should reduce the σ-effect for the 2-NH and 3-H hydrogens since the σ-mechanism is strongly dependent

(39) La Mar, G. N.; Horrocks, W. D.; Holm, R. H. Eds. In *NMR of Paramagnetic Molecules*; Academic Press: New York, 1974.
(40) (a) Kurland, R. J.; Mc Garvey, B. R. *J. Magn. Reson.* **1970**, *2*, 286. (b) Bleaney, B. J. *J. Magn. Reson.* **1972**, *8*, 91.

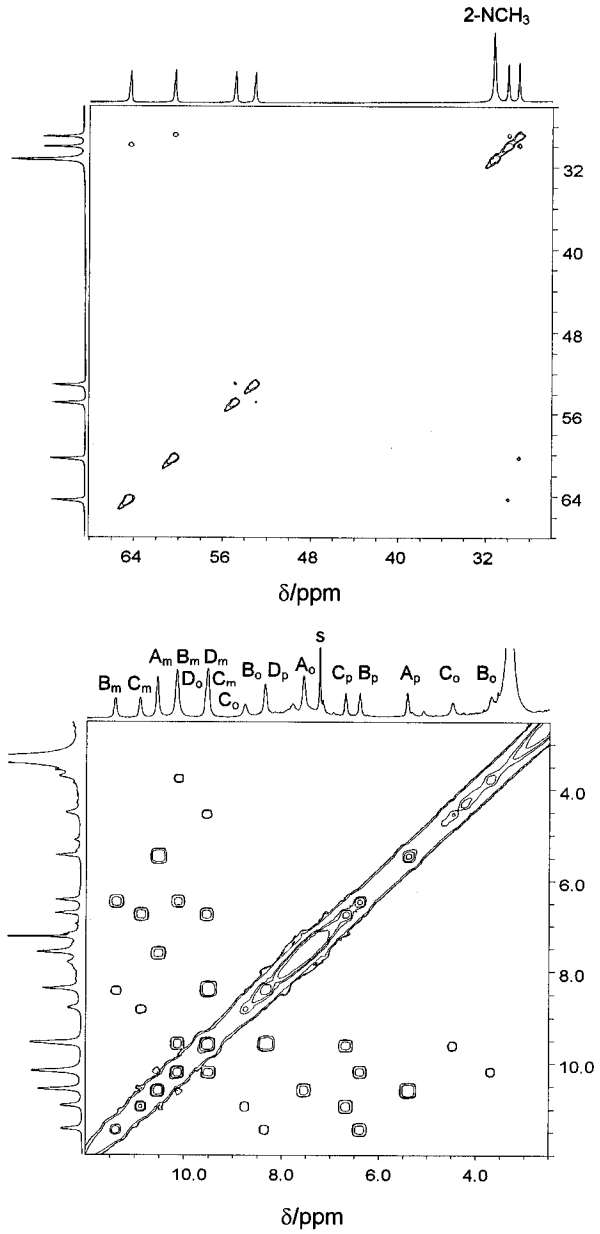

Figure 9. The 2D ^{1}H COSY spectrum of (2-NCH_3-21-CH_3CTPP)-$Ni^{II}Cl$ ($CDCl_3$, 273K). Upper map, low field region showing spin−spin coupling of regular pyrrole protons; lower map, *meso*-phenyl region; peak labels denote respective *ortho*, *meta*, or *para* protons of unequivalent phenyl rings; s, solvent.

on geometry.[41] The replacement of the upfield shifted 2-NH proton of (2-NH-21-CH_3CTPP)$Ni^{II}Cl$ with the methyl group of (2-NCH_3-21-CH_3CTPP)$Ni^{II}Cl$ results in the downfield shift of 2-NCH_3 with the similar absolute value of the isotropic shift. This demonstrates a dominance of the π-transfer mechanism at this fragment of C-methylated nickel(II) carbaporphyrin. The pattern of the six downfield pyrrole resonance shows the domination of the σ-mechanism. However a large difference in contact shifts of pyrrole resonances is seen even for protons located on the same pyrrole ring. These differences result from the π-spin density delocalized by the porphyrin framework and originating from the peculiar spin density transfer within the inverted pyrrole ring. Previously we have observed and discussed the similar π delocalization of unpaired spin density in nickel(II) heteroporphyrins and nickel(II) *N*-methylporphyrins in terms of ligand-to-metal and metal-to-ligand charge transfer.[13,16,17] The considerable differences of the spin densities at the particular pyrrole carbons were related to the pattern of the occupied π and unoccupied π* molecular orbitals.

Reaction Mechanism. Reaction of methyl iodide with (CTPP)Ni^{II} results in formation of (21-CH_3CTPP)Ni^{II} accompanied by formation of two paramagnetic derivatives (2-NH-21-CH_3CTPP)$Ni^{II}X$ and (2-NCH_3-21-CH_3CTPP)$Ni^{II}X$. The remarkable modification of the organometallic substrate results from the methylation of the inner σ-coordinating sp^2 hybridized 21-carbon atom. This transformation changes the pattern of the C(21) coordination from planar to the pyramidal one owing to the sp^3 hybridization in the C-methylated diamagnetic product (21-CH_3CTPP)Ni^{II}. The coordination of this carbon corresponds formally to the formation of a tertiary alkyl complex.[42] The unusual side-on coordination preserving strongly sp^2 trigonal geometry of 21-C has been found appropriate to describe the bonding in the paramagnetic (2-NH-21-CH_3CTPP)$Ni^{II}X$ and (2-NCH_3-21-CH_3CTPP)$Ni^{II}X$ complexes. These are the principal structural features determining the properties of these compounds which should be taken into account in the reaction mechanism. Usually, the Ni^{II}−C configuration observed in this work would be expected to be unstable, but firm restraints imposed by the location of a coordinating center inside the macrocycle provide a reason for the extraordinary stability. The first methylation step may involve either nickel(II) or negative charged nucleophilic carbon atom. Accordingly two reaction mechanisms can be suggested. Scheme 1 considers the situation that, in the transient state, the σ-methylation of nickel(II) has taken place to generate formally σ-methylated nickel(IV) species. The formation of the intermediate may be preceded by the S_{N^2} displacement of the iodide by the nickel(II) nucleophilic of the methyl iodide as suggested for methylation of $[(2,6\text{-}Me_2NCH_2)C_6H_3]Pt^{II}\}^+$.[1o] The transients will undergo 1,2-methyl shift between nickel and C-coordinated pyrrole to produce a nickel(II) complex of C-methylated carbaporphyrin. The reaction intermediate presents an oxidation state of the nickel rarely found in coordination complexes. Moreover a stabilization of Ni^{IV} with alkyl-substituted diphosphine and diarsine ligands is well established.[43] Recently (alkyl radical)-organonickel(III) complexes, formally two electrons oxidized with respect to the ground state, were considered as the plausible transient intermediates in addition to reaction of polyhalogenoalkanes to olefin catalyzed by arylnickel(II) complexes.[1h−1l] Alternatively the methyl iodide molecules interacts directly with the substrate (Scheme 2), and the oxidative addition of the methyl cation to the carbaporphyrin at the C(21) will take place. The redundant positive charge from the macrocycle may be removed by the dissociation of 2-NH proton. Coordination of iodide, which in this mechanism accompanies the bond cleavage in methyl iodide, would result in formation of the sterically unfavorable arrangement of C-methyl and axially coordinated iodide on the same side of the macrocycle. In structurally similar *N*-methylporphyrin complexes the coordination of an anion usually takes place at the opposite to *N*-methyl side of the equatorial plane unless low temperature conditions are generated.[44] For this reason we have suggested the concerted dissociation of the HX (HI, HCl) molecule to produce the diamagnetic (21-CH_3CTPP)Ni^{II} complex. We have found however that concerted HX dissociation/association is reversible according to the mechanism presented in Scheme 3. Finally as the reaction proceeds, the N(2) methylation takes place as

(41) Bertini, I.; Luchinat, C. In *NMR of Paramagnetic Molecules in Biological Systems*; The Benjamin/Cumming Publishing Co. Inc.: Menlo Park, CA, 1986.

(42) Balch, A. L.; Hart, R.; Latos-Grażyński, L.; Traylor, T. G. *J. Am. Chem. Soc.* **1990**, *112*, 7382.

(43) (a) Higgins, S.; Levason, W.; Feiters, M. C.; Steel, A. T. *J. Chem. Soc., Dalton Trans*. **1986**, 317. (b) Hanton, L. R.; Evans, J.; Levason, W.; Perry, R. J.; Webster, M. *J. Chem. Soc., Dalton Trans*. **1991**, 2039.

(44) Balch, A. L.; Cornman, C. R.; Latos-Grażyński, L.; Olmstead, M. M. *J. Am. Chem. Soc.* **1990**, *112*, 7552.

Scheme 1

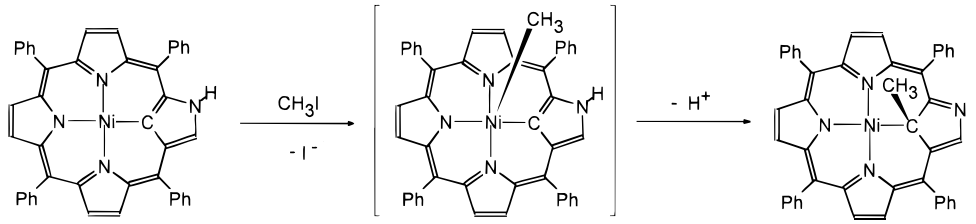

Scheme 2

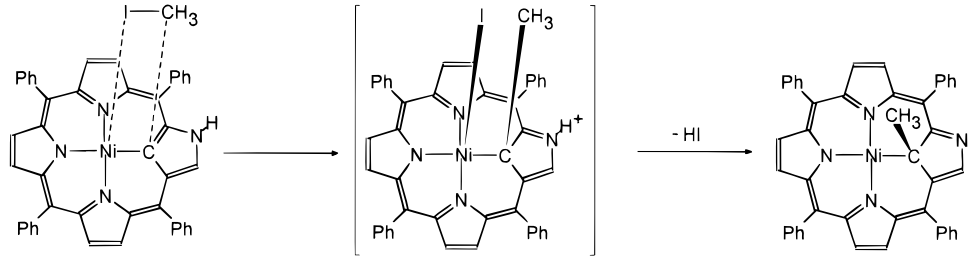

Scheme 3

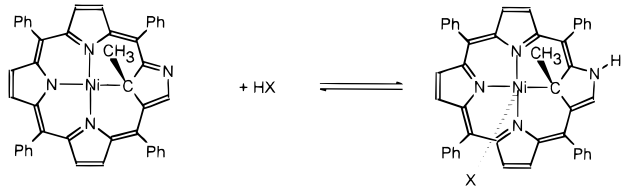

well. In this case the positive charge in the system is compensated by the strong tendency to axially coordinate of an anionic ligand.

The ionic charge of the coordination center determines the spin state of their nickel(II) complexes. The monoanionic coordination supports the paramagnetic $S = 1$ electronic state. Dianionic coordination results in the diamagnetic complexes. To the best of our knowledge this is the very first example of the control of the spin state in the organometallic nickel(II) complexes by the concerted reversible addition of the HX molecule.

Conclusions

The present work offers conclusive evidence for the stabilization of paramagnetic organometallic nickel(II) complexes *via* the very efficient protection of the nickel−carbon bond by encapsulating the coordinating carbon center in the structure of the porphyrin macrocycle. The general overview of the reactivity pattern emphasizes the unusual methylation route which includes methylation of the sp^2 hybridized coordinated C(21) atom to end up with its pyramidal or pyramidally distorted trigonal geometry for this center in the methylated species. The viability of C-methylated ligands for reversible nickel removal/insertion processes demonstrates the spectacular flexibility of the ligand electronic/molecular structure accompanied by the appropriate reversible hybridization change $sp^3 \rightleftharpoons sp^2$.

Formally the methylated pyrrolic fragments of both compounds i.e., (21-CH_3CTPP)Ni^{II} and (2-NCH_3-21-CH_3CTPP)-Ni^{II}X may be treated as structural models of the hypothetical reductive-elimination process assuming the C-methylated pyrrole as a leaving group. The macrocyclic restraints stop the process at the stage just preceeding the elimination of the methylated organic fragment. The smooth structural rearrangements, inherent to reductive-elimination, seem to be appropriately visualized by the respective "snapshot" structures of mono- and dimethylated complexes, considered here as two likely stages in the full sequence of the process (Scheme 4).

Experimental Section

Solvents and Reagents. All solvents were purified by standard procedures. Chloroform-*d* ($CDCl_3$, Glaser AG) was dried before use by passing through activated basic alumina.

Preparation of Compounds. CTPP, 2-NCH_3CTPP, and their nickel(II) complexes were synthesized as previously described.[14,16] $CTPPH_2$-d_7 was obtained in the identical procedure as $CTPPH_2$, but the regular pyrrole was replaced with pyrrole-d_5 (Aldrich).

Synthesis of 2-Aza-5,10,15,20-tetraphenyl-21-methyl-21-carbaporphyrinatonickel(II) ((21-CH_3CTPP)Ni^{II}) and 2-Aza-2,21-dimethyl-5,10,15,20-tetraphenyl-21-carbaporphyrinatonickel(II) Chloride ((2-NCH_3-21-CH_3CTPP)Ni^{II}Cl). CH_3I (1 mL, 8 mmol) was added to a solution of (CTPP)Ni^{II} (100 mg, 0.15 mmol) in dichloromethane and stirred for 24 h at 293 K. The mixture was then taken to dryness under reduced pressure. The product was dissolved in dichloromethane and chromatographed on the silica gel column with dichloromethane as an eluent. The fastest moving green band consisted of starting material (21-CH_3CTPP)Ni^{II}, the second olive band contained (21-CH_3CTPP)Ni^{II}, and the third brown band (eluted with 10% solution of chloroform in dichloromethane) was a mixture of (2-NCH_3-21-CH_3-CTPP)Ni^{II}Cl and (2-NCH_3-21-CH_3CTPP)Ni^{II}I. From the fraction containing monomethylated species (brown solution) the brown solid was obtained by addition of *n*-hexane and dried *in vacuo* for 5 days. Yield: 34 mg (33%). ^{1}H NMR (300 MHz, 293 K, $CDCl_3$) δ 9.898 (3-H), 8.633 (m, overlapping parts of two AB systems, two pyrrole protons), 8.49 (m, overlapping parts of two AB systems, two pyrrole protons, 8.452, 8.415 (AB, $^3J = 4.5$ Hz), 8.18 (b, *ortho*), 8.06 (b, *ortho*), 7.77 (m, *meta*), 7.69 (m, *para*), −3.154 (21-CH_3). UV−vis λ_{max}/nm (log ϵ) 430 (4.59), 550 (sh), 610 (sh), 735 (2.72); MS (EI, 70 eV) 684 ($[M - H]^+$, 100%), 670 (M − CH_3, 30%). Anal. Calcd for $C_{45}H_{30}N_4$-Ni: C, 78.93; H, 4.42; N, 8.19. Found: C, 78.46; H, 4.22; N, 7.78.

Chloroform solution containing dimethylated species (the third fraction) was shaken with 5% hydrochloric acid, and organic phase was then evaporated and dried. The oily product was dissolved in dichloromethane and precipitated with hexane giving 10 mg of dark green solid. ^{1}H NMR still revealed presence of about 10% of (2-NCH_3-21-CH_3CTPP)Ni^{II}I. The full *in situ* conversion to the chloride salt was accomplished by addition of 2-fold excess of tetraethylammonium chloride: UV−vis λ_{max}/nm (log ϵ) 465 (4.26), 580 (sh), 730 (3.80), 820 (sh); MS (LSIMS) 699 (M − Cl − 1). Syntheses of (21-CD_3-CTPP)Ni^{II} and (2-NCD_3-21-CD_3CTPP)Ni^{II}Cl were performed analogously using CD_3I (POCh).

Synthesis of 2-Aza-2-hydro-5,10,15,20-tetraphenyl-21-methyl-21-carbaporphyrinatonickel(II) Chloride ((2-NH-21-CH_3CTPP)Ni^{II}Cl). Solution of 2-aza-21-methyl-21-carbatetraphenylporphyrinatonickel(II) (20 mg, 0.029 mmol) in 50 mL of chloroform was stirred with 10 mL

Scheme 4

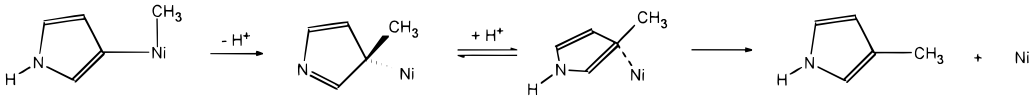

of 1% solution of hydrochloric acid until brown solution turned green. The organic layer was then separated, dried, dissolved in dichloromethane, and precipitated with hexane. Yield: 10 mg (48%). UV−vis λ_{max}/nm (log ϵ) 455 (4.54), 580 (3.35), 730 (3.88), 820 (sh). Anal. Calcd for $C_{45}H_{31}N_4NiCl\cdot CH_2Cl_2$: C, 71.77; H, 4.32; N, 7.28. Found: C, 72.00; H, 4.25; N, 6.94.

Synthesis of 2-Aza-2,21-dimethyl-5,10,15,20-tetraphenyl-21-carbaporphyrinatonickel(II) Iodide ((2-NCH$_3$-21-CH$_3$CTPP)Ni^{II}I). Solution containg (2-NCH$_3$CTPP)Ni^{II} (20 mg, 0.029 mmol) and methyl iodide (8 mmol) in 50 mL of dichloromethane was stirred for 48 h. After that time the green solution turned brown. Reaction mixture was then taken to dryness, dissolved in dichloromethane, and precipitated with *n*-hexane. Yield: 19 mg (79%). UV−vis λ_{max}/nm (log ϵ) 435 (4.26), 465 (4.27), 575 (sh), 670 (sh), 735 (3.85). Anal. Calcd for $C_{46}H_{33}N_4NiI\cdot CH_2Cl_2$: C, 61.88; H, 3.87; N, 6.14. Found: C, 62.32; H, 4.15; N, 6.29.

Synthesis of 2-Aza-5,10,15,20-tetraphenyl-21-methyl-21-carbaporphyrin (21-CH$_3$CTPPH$_2$). Solution of (21-CH$_3$CTPP)Ni^{II} (20 mg, 0.029 mmol) in 50 mL of dichloromethane was shaken with 10% hydrochloric acid. After solution color turned green, the water layer was removed, and organic layer was washed with water and dried with sodium carbonate. Chromatography on a basic alumina column with dichloromethane as an eluent (brown-green band was collected) and crystallization from dichloromethane/ethanol gave 10 mg (55%) of the free carbaporphyrin: ^{1}H NMR (300 MHz, CD_2Cl_2, 203 K) δ 8.979, 8.490 (AB, ^3J = 4.6 Hz), 8.821, 8.418 (AB, ^3J = 4.7 Hz), 8.463 (m, 2H) (regular pyrrole protons), 8.664 (d), 8.274 (d), 8.202 (d), 8.55 (b), 8.32 (b), 8.002 (d) (*ortho*), 8.06−7.75—overlapping multiplets of *meta* and *para* protons, 7.113 (3-H), −3.014, −3.195 (22, 24-NH), −4.837 (3H, 21-CH$_3$). Assignments were made on the basis of 2D COSY experiment: UV−vis λ_{max}/nm (log ϵ) 445 (4.96), 515 (3.72), 550 (3.94), 590 (4.02), 740 (3.95); MS (EI, 70 eV) 630 (100%, M + 1). Anal. Calcd for $C_{45}H_{32}N_4\cdot CH_2Cl_2\cdot C_2H_5OH$ (the presence of solvents detected in the ^{1}H NMR spectrum): C, 79.60; H, 5.57; N, 7.74. Found: C, 79.77; H, 5.19; N, 7.85.

Synthesis of 2-Aza-2,21-dimethyl-5,10,15,20-tetraphenyl-21-carbaporphyrin (2-NCH$_3$-21-CH$_3$CTPPH). Solution of (2-CH$_3$-21-CH$_3$-CTPP)Ni^{II}I (20 mg, 0.024 mmol) in 50 mL of dichloromethane was stirred with concentrated hydrochloric acid for 1 h. Acid was then removed and organic phase was washed with water and dried with sodium carbonate. Product was chromatographed on a basic alumina column with dichloromethane as an eluent. The fastest moving green band was collected. Addition of ethanol to the solution and reduction of solvents volume resulted in deep green precipitate. Yield: 8 mg (51%). ^{1}H NMR (300 MHz, CD_2Cl_2, 203 K) δ 7.910, 7.27 (AB, ^3J = 4.4 Hz), 7.845, 7.27 (AB, ^3J = 4.4 Hz), 7.59 (m, 12,13-H) (regular pyrrole protons), 8.06 (m, 2H), 8.00 (m, 2H) (*ortho* protons), 7.79−7.54 (overlapping multiplets of *meso*-phenyl protons), 5.647 (3-H), 3.824 (23-NH), 2.905 (2-CH$_3$), −1.584 (21-CH$_3$). Assignments based on selective proton-decoupling: UV−vis λ_{max}/nm (log ϵ) 455 (4.90), 600 (sh), 655 (4.15), 710 (4.25); MS (EI, 70 eV) 644 (100%, M + 1). Anal. Calcd for $C_{46}H_{34}N_4\cdot CH_2Cl_2\cdot C_2H_5OH$ (the presence of solvents detected in the ^{1}H NMR spectrum): C, 76.06; H, 5.47; N, 7.24. Found: C, 76.45; H, 5.13; N, 7.31.

Instrumentation. ^{1}H NMR spectra were recorded on a Bruker AMX spectrometer operating in the quadrature mode at 300 MHz. A typical spectrum was collected over 45 000 Hz (paramagnetic systems) or 4500 Hz (diamagnetic compounds) spectral window with 32 K data points with 100−5000 transients for the experiment and 50 ms (paramagnetic) or 2 s (diamagnetic samples) prepulse delay. The free induction decay (FID) was apodized using exponential multiplication depending on the natural line width. This induced 0.2−30 Hz broadening. The residual ^{1}H NMR resonances of the deuterated solvents were used as a secondary reference. The ^{2}H NMR spectra were collected using a Bruker AMX instrument operating at 46.1 MHz. A spectral width of 20 kHz was typical, and 16 K points were used. A pulse delay of 50 ms was applied. The signal-to-noise ratio was improved similarly as in proton spectra. The residual ^{2}H NMR resonances of the solvents were used as a secondary reference.

The 2D COSY spectra were obtained after collecting a standard 1D reference spectrum. The 2D spectra were collected by use of 2048 points in t_2 over the desired bandwidth (to include all desired peaks) with 512 t_1 blocks and 320 scans per block. All experiments included four dummy scans prior to the collection of the first block. Absorption spectra were recorded on a Spekord M-42 spectrometer and diode array Beckman 7500 spectrometer. Mass spectra were recorded on a ADM-604 spectrometer using the liquid matrix secondary ion mass spectroscopy (8 keV Cs^+ ions) or electron impact techniques.

X-ray Data Collection and Refinement (21-CH$_3$CTPP)Ni^{II}·CH$_2$-Cl$_2$. Crystals of (21-CH$_3$CTPP)Ni^{II} were prepared by diffusion of *n*-hexane into the dichloromethane solution contained in a thin tube. Data were collected at 293 K on a Kuma KM-4 diffractometer. The stability of intensities was monitored by the measurement of three standards every 100 reflections. The data were corrected for Lorentz and polarization effects. No absorption correction was applied. Crystal data are compiled in Table 4.

The structure was solved by the direct methods with SHELXS-86 and refined by full-matrix least square method using SHELX-93 with anisotropic thermal parameters for non-H atoms. Scattering factors were those incorporated in SHELXS-93.

The disorder at the N(2)−C(3) positions was treated by examining several different models which exchange N(2) and C(3) atoms. The last cycles of refinement include N(2) and N(3′) at 50% occupancy. The positional parameters of these atoms were fixed and their isotropic thermal parameters allowed to vary. A molecule of dichloromethane in the lattice exhibits a disorder.

(2-NCH$_3$-21-CH$_3$CTPP)Ni^{II}I·C$_6$H$_6$. The suitable crystals of (2-NCH$_3$-21-CH$_3$CTPP)Ni^{II}I were prepared by diffusion of *n*-hexane into the benzene solution contained in a thin tube. Data were collected at 293 K on a Kuma KM-4 diffractometer. The stability of intensities was monitored by the measurement of three standards every 100 reflections. The data were corrected for Lorentz and polarization effects. No absorption correction was applied. Crystal data are compiled in Table 4.

The structure was solved by the direct methods with SHELXS-86 and refined by full-matrix least square method using SHELX-93 with anisotropic thermal parameters for non-H atoms. Scattering factors were those incorporated in SHELXS-93. The disorder at the N(2)−CH$_3$ positions was treated by examining several different models which exchange N(2)−CH$_3$ and C(3)−H groups. The last cycles of refinement include N(2)−C(26) at 65% occupancy and N(3′)−C(27) at 35% occupancy.

Acknowledgment. The financial support of the State Committee for Scientific Research KBN (Grant 3 T09A 14309) is kindly acknowledged.

Supporting Information Available: Crystal data, atom coordinates, complete listings of bond lengths, anisotropic displacement coefficients, and calculated hydrogen parameters (20 pages). Ordering information is given on any current masthead page.

JA9527028